USDA FOREST SERVICE
RESEARCH PAPER NC-105
1974

DESIGN of thin shear blades for crosscut shearing of wood

Rodger A. Arola, Thomas R. Grimm

NORTH CENTRAL FOREST EXPERIMENT STATION
FOREST SERVICE
U.S. DEPARTMENT OF AGRICULTURE

CONTENTS

THE AUTHORS: Rodger A. Arola is a Principal Mechanical Engineer at the Station's Forest Engineering Laboratory in Houghton, Michigan. The Laboratory is maintained in cooperation with Michigan Technological University. Thomas R. Grimm is a Computer Applications Analyst for the Union Carbide Corporation, Nuclear Division, Oak Ridge, Tennessee.

North Central Forest Experiment Station
John H. Ohman, Director
Forest Service - U.S. Department of Agriculture
Folwell Avenue
St. Paul, Minnesota 55101
(Maintained in cooperation with the University of Minnesota)

Manuscript approved for publication November 23, 1973

DESIGN OF THIN SHEAR BLADES FOR CROSSCUT SHEARING OF WOOD

Rodger A. Arola and Thomas R. Grimm

BACKGROUND

During the early 1960's one major obstacle that designers of wood harvesting equipment had to overcome was the lack of information on force and power requirements for crosscut shearing of wood. Over the last 10 years reliable information has been published. However, throughout this 10-year period we have not witnessed widespread acceptability of shear-felled sawtimber as we have with shear-felled pulpwood. Why? The major deterrent has been the splitting of the butt saw log which causes severe monetary losses in the production of lumber.

McIntosh and Kerbes (1968) found that shearing trees reduced felling costs of conventional methods by 37.9 percent in a clearcut lodgepole pine stand and by 48.5 percent in Douglas fir. However, the butt log split an average of 10 inches in the lodgepole pine causing an estimated trim loss of 3 fbm per tree. A thinner shear blade reportedly used on the Douglas-fir limited splitting damage to 4 to 5 inches and crushing damage 1 to 2 inches from the sheared face. All material was unfrozen. Schmidt and Melton (1968) concluded that the type of tree shear they investigated was "not the ultimate machine for use in felling saw log trees."

Research has shown that splitting damage as well as force and power requirements can be decreased by using thinner shear blades (Arola 1971, 1972). But, how thin can we make functional shear blades? Thin shear blades are extremely prone to lateral buckling due to the presence of compressive stresses within the plane of the blade (in addition to unbalanced lateral pressures)(fig. 1).

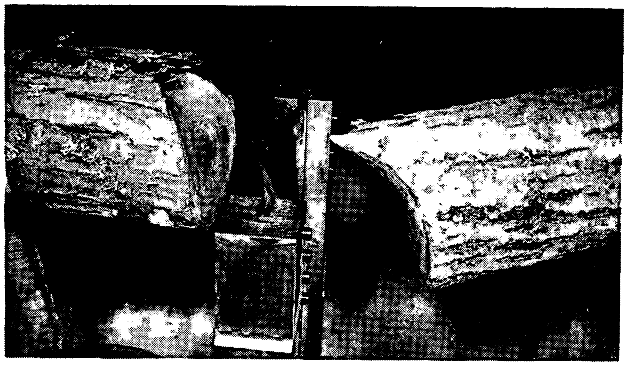

Figure 1.--*Buckled thin shear blade after crosscut shearing a 6-inch diameter oak bolt. Blade thickness is 1/8-inch $B/A \simeq 1.0$.*

The problem is further complicated by the fact that conventional "thick or deep beam" analysis does not apply to thin plates subjected to beam-type loadings. One standard assumption in the analysis of deep beams is that plane sections before stressing remain plane after stressing within the elastic range. This assumption, however, is an oversimplification for shear blades having the dimensions of a thin plate rather than a beam. Elasticity theory must be used to determine the stress distributions resulting from beam-type loadings, and complicated plate theory used to determine the critical buckling load or stress which causes failure.

The literature revealed limited information about methods to predict the elastic stability of thin plates subjected to in-plane loadings. Prestressing can be used to increase the stability of thin plates, but information is also limited on prestressed plates or shear blades.

Despite the lack of theoretical information about the design of thin shear blades there are reports of experimental tests using thin prestressed shear blades. Wiklund (1967) demonstrated the beneficial effect of prestressing shear blades and tested a 10 mm- (0.4 in.) thick blade to shear wood 20 to 25 cm (8 to 10 in.) in diameter. In his analysis he treated the thin blade stress distribution similar to that in deep beams subjected to the same loadings. He used a mechanical test arrangement to prestress the shear blade while the stress level was monitored with strain gages. Wiklund also cited field tests conducted in Russia with two opposing prestressed, 5 mm- (0.2 in.) thick blades to shear frozen trees up to 70 cm (≈28 in.) in diameter. Cuts were very smooth with little splitting damage. So, there is an advantage in using thin shear blades to reduce splitting damage and the force needed, and being able to predict increases in blade stability by prestressing.

The Forest Engineering Laboratory therefore initiated an analytical study which led to the development of a versatile computer program for thin plate analysis. (Appendix A). The program was used to solve instability problems of edge-loaded thin plates having several possible shear blade configurations and three different prestress methods, as well as numerous other thin rectangular plate instability problems to which some solutions were previously nonexistent.

PURPOSE

The purpose of this paper is: (1) to present a measure of stability for establishing critical buckling loads for thin rectangular plates which have different depth/width (B/A) or aspect ratios and clamping (boundary) conditions and are subjected to different in-plane compressive loads (see Appendix B for explanation of symbols); (2) to indicate the possible increase in plate stability by applying alternative in-plane prestress loadings; and (3) to exemplify how a designer could use this information to determine whether the critical buckling load will be reached with the expected shear loads, and how prestressing can increase blade stability.

PLATE CONFIGURATIONS ANALYZED

Numerous basic configurations of thin rectangular plates were analyzed. Those which are approximations to thin shear blades are discussed in the body of this paper. The general plate solutions, some of which were previously unsolved, are included in Appendix C.

The primary plate dimensions and coordinate system, the assumed crosscut shear loads, and the prestress configurations were all treated in this analysis (fig. 2). The main crosscut shear load assumed was a cosine-shaped, in-plane distributed load. However, a uniformly distributed load was also analyzed and a relationship developed between the two. These compressive loads which cause instability are considered to be applied to the top edge of the plates with no lateral pressure or perturbation. The in-plane prestress distributions include a uniform tension, a linearly increasing tension, and a bending moment-type stress distribution applied to the vertical edges of the plates.

The plate boundary conditions include clamped and free edges. Additionally, some of the solutions presented in Appendix C include plates with simply supported edges, and/or combinations of simply supported, clamped, and free edges.

The clamped boundary condition indicates that the edge is restrained with respect to deflection and rotation out of the plane of the plate. The simply supported boundary condition indicates that the edge is restrained with respect to deflection out of the plane of the plate but not with respect to rotation.

Some of the plates considered are also assumed to be supported at the bottom edge by a rigid, clamped support. It is assumed that this type of support results in a compressive stress distribution applied to the bottom edge of the plate indentical to the shear load applied to the top edge (fig. 2c).

GENERAL DISCUSSION

The theory used in this work is accurate only for thin rectangular plates made of a linearly elastic, homogeneous, isotropic material. The theory can be applied to thicker plates, but with less accuracy. As a rule of thumb a plate is classified as thin if the ratio L/t is greater than 20, where L is the smaller of the two primary dimensions (A and B) and t is the plate's thickness.

The stability of a thin plate is measured in terms of a critical buckling

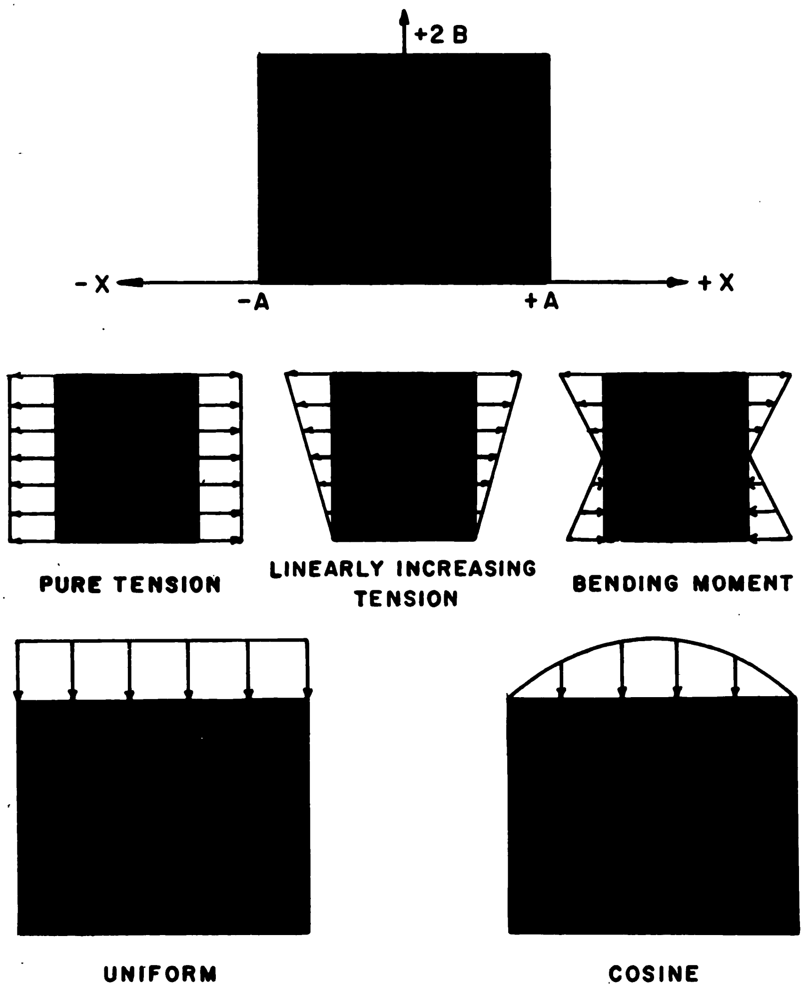

Figure 2.--*Cases treated in thin plate (shear blade) analysis: (A) plate dimensions and coordinate system; (B) prestress configurations analyzed; and (C) assumed shear load configurations analyzed.*

stress which is defined as the lowest value of the midplane stress or stresses for which the initially flat plate has two equilibrium configurations. The two equilibrium configurations are the initial flat configuration and an adjacent infinitesimally deflected configuration. The critical buckling stress establishes where the plate is at a neutrally stable configuration. It is theoretically possible for a plate to remain in its initially flat configuration despite the fact that the in-plane compressive stress exceeds the critical buckling stress. However, the flat configuration is unstable once this stress is reached. Any slight perturbation would cause the plate to buckle.

The critical buckling stress for a given plate configuration is formulated by

$$\sigma_{cr} = \frac{(CKA)\pi^2 D}{t(2A)^2} \text{ or } \frac{(CKB)\pi^2 D}{t(2B)^2}$$

where D is the flexural rigidity of the plate, t is the thickness of the plate, A is one half the plate width in the X direction, CKA is the buckling constant for the A dimension, B is one half the plate depth in the Y direction, and CKB is the buckling constant for the B dimension.

Either of the above expressions make it possible to determine the critical buckling stress for thin plates which have different dimensions and material constants but which are loaded and supported in the same manner and have the same aspect ratio B/A. The buckling constant is independent of material constants for plates having all edges supported. The material properties are accounted for in the flexural rigidity term (D) which is given as

$$D=\frac{Et^3}{12(1-\mu^2)}$$

in which E is the modulus of elasticity, t is the plate thickness, and μ is Poisson's ratio. However, if the plates considered have a free edge or edges, the buckling constant is dependent on Poisson's ratio. For cases with free edges it is therefore necessary to specify the Poisson ratio, along with the buckling constant for a given problem. A value of 0.3 (for steel) has been assumed throughout this analysis.

The prestress distribution analytically applied to the thin plates were expressed in a form similar to that of the buckling constant described above. The peak value of the prestress (PPS) was expressed in terms of a prestress factor (PK), multiplied by the plate stress constant (σ_e). Thus,

$$PPS=(PK)\sigma_e \text{ where,}$$

$$\sigma_e=\frac{\Pi^2 D}{t(2A)^2}.$$

The peak prestress was expressed in the above form so that the numerical results obtained from the instability analysis of the prestressed plates can be applied to other plates with the same aspect ratio but different dimensions and material constants. The effectiveness of the prestress was measured in terms of the increase in the magnitude of the critical buckling stress.

RESULTS

Comparison Between Uniform and Cosine Load Distributions

Most results presented are for plates analyzed with a cosine-type load distribution which, as an oversimplification, was assumed to approximate the blade load due to crosscut shearing of logs. However, the critical buckling stress for several of the same basic plate configurations, but with a uniformly distributed load, was also analyzed. It was found that the total force which will cause buckling for the assumed cosine distributed load (P_c) was less than the total force which will cause buckling for a uniformly distributed load (P_u). This, we believe, is because the cosine-shaped distributed load in effect "wastes" less force near the restrained edges of the plate. The relationship between the total loads for the two assumed load distributions for plates having both clamped and simply supported vertical edges is shown in figure 3.

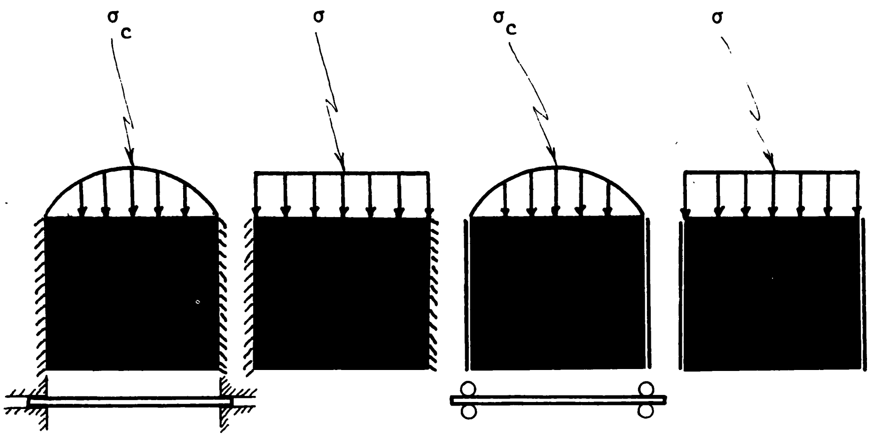

Figure 3.--*Relationship between uniform and cosine distributed buckling loads for clamped thin plates (left) ($P_c \simeq 0.70\ P_u$) and simply supported thin plates (right) ($P_c \simeq 0.75\ P_u$). Where $P_c = {}_0\int^A \sigma_c\, dA = \frac{2}{\pi}(2A)\, t\sigma_c$; and $P_u = {}_0\int^A \sigma\, dA = (2A)\ t\ \sigma$.*

Knowing the total cutting force for a given species and diameter of tree, the results of the instability analysis presented here can relate this cutting force to the peak value of stress. For example, the total force for a cosine distributed load (fig. 3) is

$$P_c = \frac{2}{\pi}(2A)\,t(\sigma_c).$$

The peak stress is therefore given by

$$\sigma_c = \frac{\pi}{2}\left(\frac{P_c}{(2A)\,t}\right) \text{ or,}$$

$$\sigma_c = \frac{\pi}{2}\sigma_{avg}, \text{ where}$$

$$\sigma_{avg} = \frac{P_c}{(2A)\,t}.$$

Thus, the peak stress for the cosine distributed load (σ_c) is found by multiplying the average stress by a factor $\pi/2$ or 1.5708.

If the cutting force were initally assumed to be uniformly distributed on the blade edge and caused buckling, it can be related to the critical buckling stress for cosine-shaped loads. For example, in the case of *two clamped vertical edges* (fig. 3), the total buckling force for the cosine load is equal to $\simeq$ 0.7 times the total force for a uniform load[1] Also, since

$$2At = \frac{\pi}{2}\frac{P_c}{\sigma_c} \quad \text{and}$$

$$2At = \frac{P_u}{\sigma_u},$$

these two expressions can be set equal to each other, i.e.

$$\frac{\pi}{2}\frac{P_c}{\sigma_c} = \frac{P_u}{\sigma_u}.$$

[1] *T. R. Grimm. Analysis of the instability of thin rectangular plates using the extended Kantorovich method. (Unpublished Ph.D. dissertation on file at Mich. Technol. Univ., Houghton, Mich.) 1972.*

Substituting 0.7 P_u for P_c and solving for σ_u results in the following expression:

$$\sigma_u = 0.9094\,\sigma_c.$$

Thus, the critical buckling stress for a thin plate having two clamped vertical edges and a uniformly distributed load can be approximated by multiplying the critical stress for the plate with a cosine load by a factor of 0.9094. A relationship can also be derived for the simply supported boundary condition.

Plates Without Prestressing

Two cases of plate instability illustrate the type of problems that can be solved (fig. 4). Case 1 is a thin plate with a cosine-shaped in-plane load distributed along an otherwise free top (cutting) edge. The vertical edges of the plate are rigidly clamped with respect to rotations and deflections out of the plane of the plate, and are supported by shear forces. The instability in this case is caused by a combination of the compressive stress applied to the top edge and the bending-type stresses in the plane of the plate near the top edge. As the aspect ratio B/A increases, the magnitude of the buckling constant increases until B/A=2.0 (fig. 5, case 1). This plot reveals that for a shear blade loaded and supported as shown for case 1 (fig. 5), it would be wise from a stability standpoint to use a blade with an aspect ratio of at least one. Any further increase in aspect ratio does not yield large increases in the buckling constant.

Case 2 in figure 4 is that of a plate with a rigidly clamped bottom edge as well as clamped vertical edges. Again, the plate is loaded with a cosine-shaped distributed load applied to the top edge but in this case the load is resisted by the bottom edge. The instability is caused by the in-plane compressive stresses in the vertical direction, without any effect of horizontal stresses caused by bending as in case 1. Because there are no bending stresses, the buckling constant is highest for a plate with a small aspect ratio. As the aspect ratio increases, the buckling constant decreases until B/A=1.5 (fig. 4; also fig. 5, case 2). A comparison reveals that case 2 has a consistently higher buckling constant than case 1 and is thus more stable.

CASE NO.	PLATE CONFIGURATION	ASPECT RATIO B/A	CRITICAL BUCKLING CONSTANT CKA
1	COSINE DISTRIBUTED LOAD 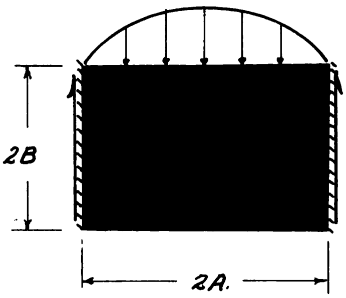	0.25	1.57461
		0.33	2.00768
		0.50	2.81051
		0.67	3.33195
		1.00	3.82011
		1.50	3.92528
		2.00	3.94223
		3.00	3.94124
2	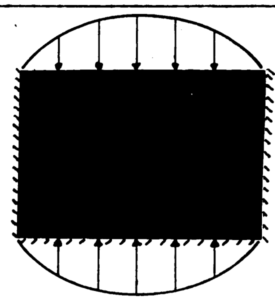	0.25	6.87814
		0.50	4.84455
		0.75	4.68299
		1.00	4.46835
		1.50	4.42998
		2.00	4.45487

Figure 4.--*Buckling constants for two thin rectangular plates approximating shear blade configurations*[1]

Plates With Prestressing

Plates having the same boundary conditions as those in figure 4, with B/A=1.0, were also analyzed to evaluate three different types of superimposed prestress distributions to increase the blade stability (fig. 6). The in-plane prestress distributions studied include a pure tension, a linearly increasing tension, and a bending moment distribution. A comparison of the magnitudes of the buckling constants with varying prestress factors reveal the effect of these three different prestress distributions on plate stability. The buckling constants were plotted against the prestress factors for the different prestress distributions (fig. 7). In both blade configurations the uniform tension prestress is the most effective for raising the critical buckling stress, the amount of stress that must be reached before buckling will occur. The triangular-shaped prestress is the second most effective, followed by the bending moment distribution.

HOW CAN A DESIGNER USE THIS INFORMATION?

In the following examples of how to use the design information, ideal plate loading and clamping conditions are assumed. The major assumption is that there is no lateral perturbation pressure which would decrease the in-plane load capacity of the blade. In actuality, when thin plates are used as shear blades, conditions are far from ideal. At the start of the actual cut it is unlikely that blade penetration is exactly perpendicular to the fibers--particularly if the cut is made close to the root collar or to a limb juncture. This failure to achieve pure orthogonal cutting conditions causes a lateral pressure on the blade which would increase

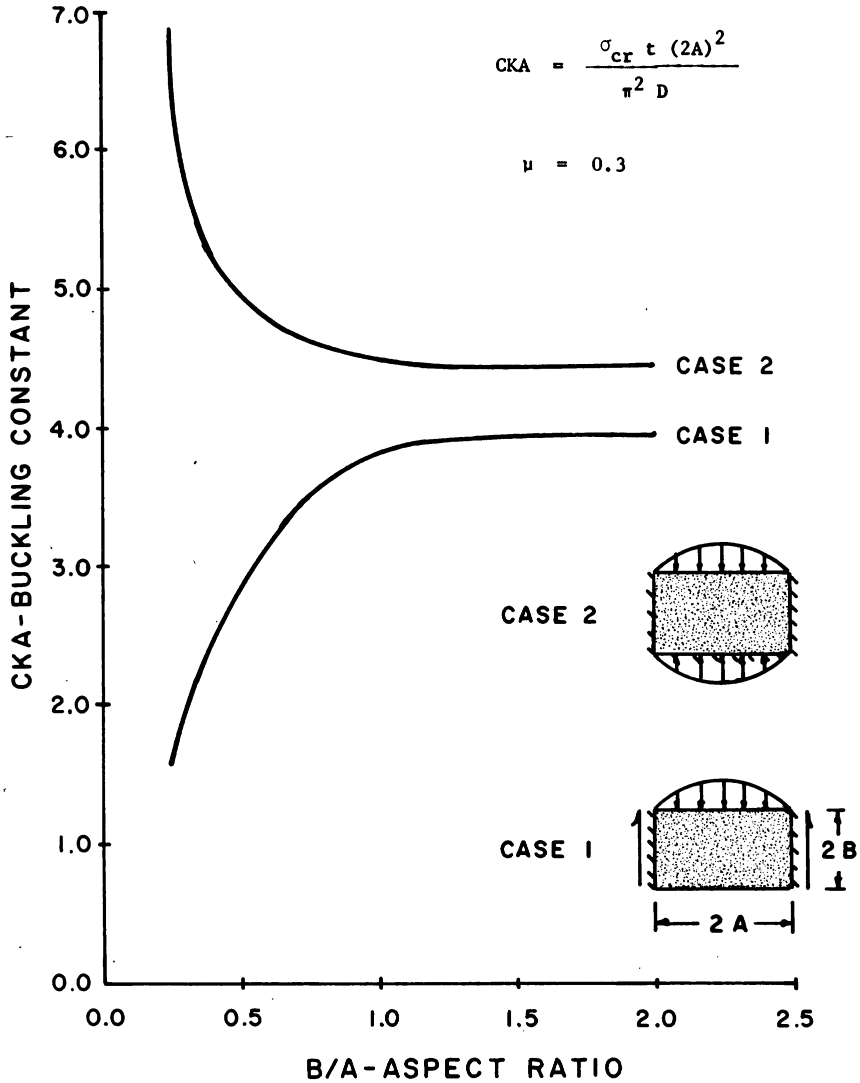

Figure 5.--*Plot of buckling constant vs. aspect ratio for two shear blade configurations*[1]

with penetration as the cutting edge tries to follow the path of least resistance along the fiber lines. Other factors affecting blade performance are misalignment of the blade or plate-containing mechanism, repeated loading, low operating temperatures, and the effect of blade imperfections. If the plate is not flat at the start, the critical buckling stress will be lower.

Because of these factors, the examples below may give theoretical in-plane buckling loads higher than those that actually cause plate or shear blade failure in the field. Nevertheless, we feel the analysis is still useful for preliminary design stages.

Example 1

It will first be assumed that the design engineer has established that his trial shear blade configuration is most closely approximated by sketch A and the plate simplification by sketch B (fig. 8). The L/t ratio is slightly greater than 20 which classifies the plate as "thin."

PRE-STRESS FACTOR	TYPE OF PRESTRESS: PURE TENSION	LINEARLY INCREASING TENSION	BENDING MOMENT
CASE 1	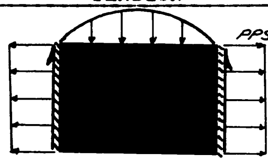	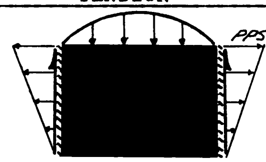	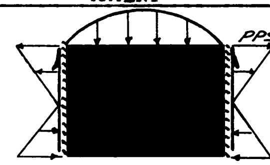
PK	CKA	CKA	CKA
0.0	3.82011	3.82011	3.82011
1.0	4.16841	4.13967	4.10945
2.0	4.46377	4.41270	4.35567
3.0	4.72814	4.65817	4.57458
4.0	4.96946	4.88252	4.76775
CASE 2	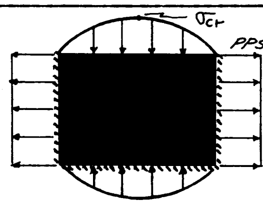	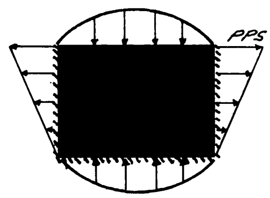	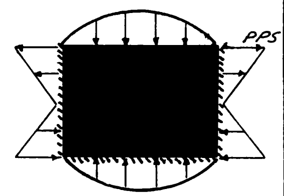
0.0	4.46835	4.46835	4.46835
1.0	4.73063	4.69595	4.65917
2.0	4.97107	4.90410	4.82733
3.0	5.19612	5.09831	4.96290
4.0	5.40748	5.30128	5.20825

Figure 6.--*Buckling constants for prestressed shear blades*[1] *(B/A = 1.0).*

We will assume the design engineer is interested in a blade without prestressing if possible, but is ready to consider adding a uniform prestress to increase the buckling constant for the assumed configuration. The following steps illustrate his checkout procedure.

The flexural rigidity (D) is first calculated for the blade.

$$D=\frac{Et^3}{12(1-\mu^2)}$$

$$=\frac{(30 \times 10^6)(0.375)^3}{12(1-0.3^2)}$$

$$D=144{,}875 \text{ in.-lb.}$$

The critical buckling stress (σ_{cr}) is then computed (for cosine distributed load):

$$\sigma_{cr}=\frac{(CKA)\pi^2 D}{t(2A)^2}$$

$$=\frac{(2.81051)(3.1416)^2\ (1.44875\text{x}10^5)}{(0.375)(18)^2}$$

$$\sigma_{cr}=33{,}075 \text{ psi .}$$

The expected crosscut shearing stress under actual cutting conditions must now be determined. A nomograph (fig. 9) can be used to estimate force requirements for

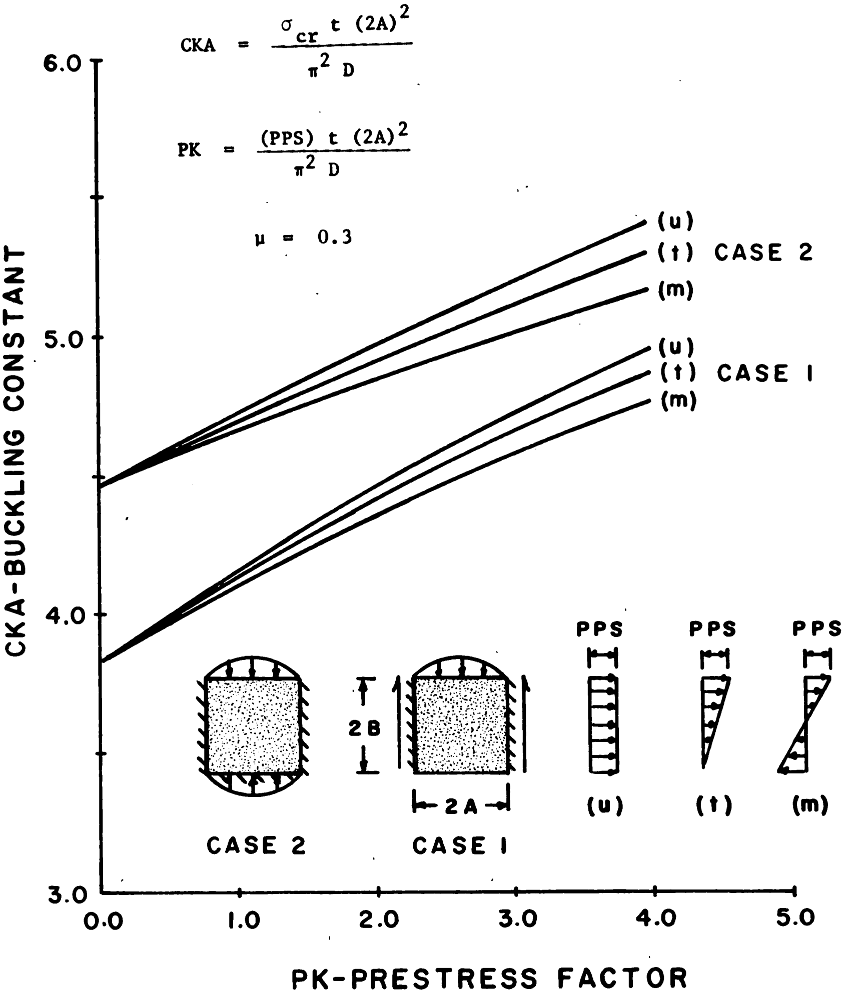

Figure 7.--*Plot of buckling constant vs. prestress factor*[1] *Prestress distributions are uniform (u), triangular (t), and bending moment (m). (B/A = 1.0).*

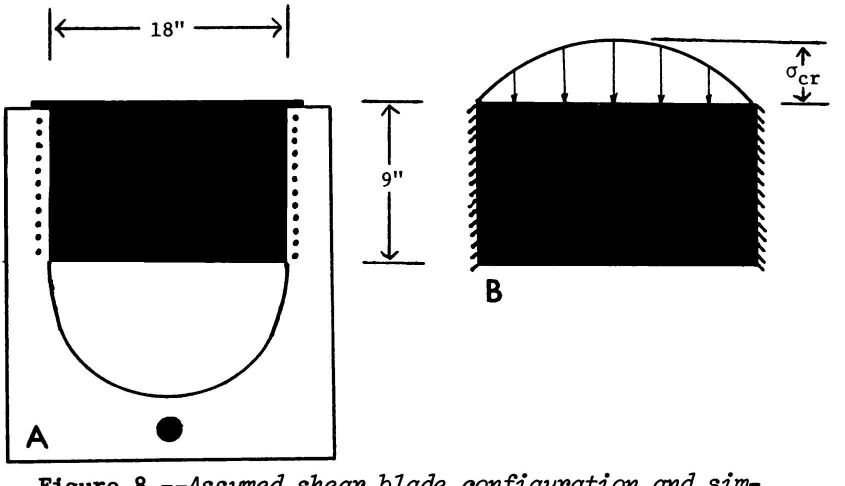

Figure 8.--*Assumed shear blade configuration and simplified rectangular plate which most closely approximates this configuration. (For case A: t = 3/8 inch, E = 30 x 10^6 psi, and μ = 0.3; for case B: B/A = 0.5, and CKA = 2.81051 (from fig. 4 case 1)).*

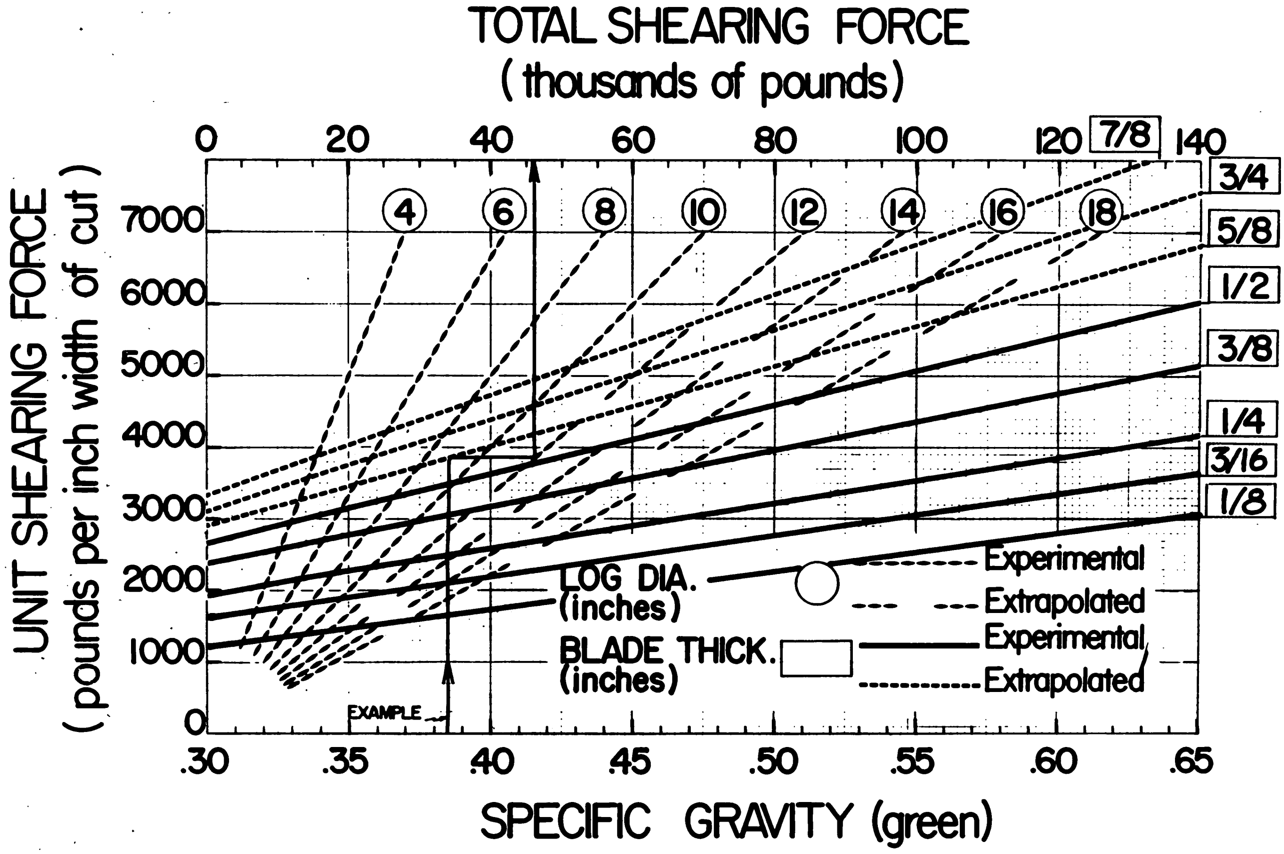

Figure 9.--*Nomograph to estimate shearing force for different blade thicknesses.*

shearing unfrozen species ranging in specific gravity (green) from 0.30 to 0.65, for log diameters up to 18 inches, and blade thickness from 1/8 inch to 7/8 inch (Arola 1972). In this example it will be assumed that the specific gravity of the material to be sheared is 0.50. From the nomograph, the total shearing force is estimated to be 72,000 pounds. To determine the average crosscut shearing stress (σ_{avg}), it is assumed that the total shearing load is distributed uniformly over the thickness and width of the blade (this is contrary to the assumed cosine distribution of figure 3; however, a correction will be made):

$$\sigma_{avg}=\frac{\text{total shearing force}}{t(2A)}\text{, or}$$

$$\frac{\text{unit shearing force}}{t}\text{ ,}$$

$$=\frac{72{,}000}{(0.375)(18)}\text{ , so}$$

$$\sigma_{avg}=10{,}667 \text{ psi.}$$

This average shearing stress must now be adjusted to correspond to a peak shearing stress value (σ_c) for a cosine distributed load. Thus, from the previous discussion,

$$\sigma_c=1.5708(\sigma_{avg})$$

$$=(1.5708)(10{,}667)$$

$$\sigma_c=16{,}755 \text{ psi.}$$

Elastic buckling occurs if $\sigma_c > \sigma_{cr}$.

From these calculations the blade is elastically stable, thus prestressing is not necessary.

Example 2

This example will illustrate a blade configuration that is not elastically stable and how the stability can be increased by changing the support conditions and by adding a uniform prestress of varying magnitudes.

It is first assumed that an 18 by 18 inch (B/A=1.0), 1/4-inch thick blade will be used (to reduce log splitting damage). The L/t ratio for this plate is much greater than 20 and definitely is classed as a thin plate. Further, it is assumed that hard maple up to 18 inches in diameter will be sheared (green specific gravity = 0.65).

The flexural rigidity of the blade is first calculated:

$$D=\frac{Et^3}{12(1-\mu^2)}$$

$$=\frac{(30\times10^6)(0.25)^3}{12(1-0.3^2)}$$

$$D=42{,}926 \text{ in.-lbs .}$$

In the calculations to follow for prestressed shear blades, the uniform prestress magnitudes are incremental values of the plate stress constant. Thus,

$$PPS=PK(\sigma_e) \ ,$$

where PK takes on values of 0.0, 1.0, 2.0, 3.0, and 4.0. The plate stress constant is calculated as

$$\sigma_e=\frac{\pi^2 D}{t(2A)^2}$$

$$=\frac{(3.1416)^2\ (42{,}926)}{(0.25)(18)^2}$$

$$\sigma_e=5{,}230 \text{ psi .}$$

Three different blade configurations are used in this example (fig. 10). Case A is a simply supported plate with two edges loosely contained in a slotted assembly (contained edges are free to rotate) and the bottom edge has no restraint. In case B, the blade is rigidly contained along the two vertical edges and the bottom edge is free. This case also considers the addition of an alternative uniform prestress of varying magnitudes. For case C, a rigid support along the bottom edge is added. The critical buckling constants are tabulated for each alternative plate configuration and prestress factor (fig. 6).

From the nomograph (fig. 9), the total shearing force for a 1/4-inch blade is estimated to be 75,000 pounds for an 18-inch-diameter hard maple tree (sp. gr. = 65). The estimated average crosscut shearing stress is calculated as

$$\sigma_{avg}=\frac{75{,}000}{(0.25)(18)}$$

$$\sigma_{avg}=16{,}667 \text{ psi .}$$

This average stress is adjusted to a peak shearing stress for a cosine distributed load. Thus,

$$\sigma_c=1.5708(\sigma_{avg})$$

$$=1.5708(16{,}667)$$

$$\sigma_c=26{,}180 \text{ psi .}$$

For each alternative combination in fig. 10 the critical buckling stress is calculated from

$$\sigma_{cr}=\frac{(CKA)\pi^2 D}{t(2A)^2} \ .$$

A comparison between the critical buckling stress and expected crosscut shearing stress reveals whether the blade will buckle elastically. Thus, if

$$\sigma_c>\sigma_{cr} \ ,$$

elastic buckling is expected.

Based on this comparison of the calculated peak stress value (σ_c=26,180 psi) with the critical buckling stresses it is apparent that both cases A and B are unsatisfactory and buckling would occur under the stated conditions. For case C, the plate is determined to be elastically stable with a prestress factor slightly greater than 2.0.

Several factors were previously discussed which would affect blade performance. Additionally, this design selection does not consider the effect of repeated loading close to the critical buckling stress. It would be desirable to have a "critical buckling fatigue limit" based on repeated

CASE	Prestress Factor PK	Critical Buckling Constant CKA	Critical Buckling Stress σ_{cr} (psi)
A 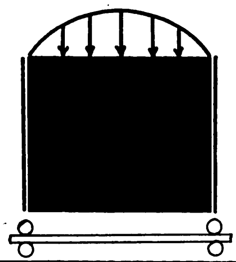	0.0	2.10034	10,985
B 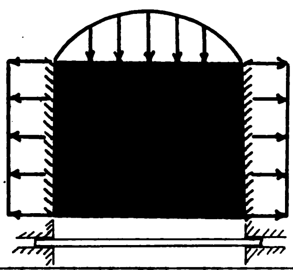	0.0	3.82011	19,980
	1.0	4.16841	21,800
	2.0	4.46377	23,345
	3.0	4.72814	24,730
	4.0	4.96946	25,990
C 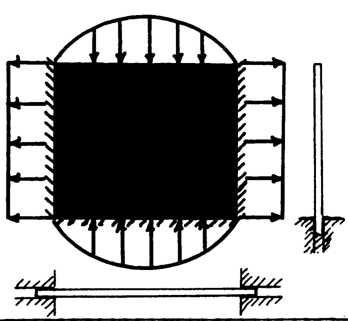	0.0	4.46835	23,370
	1.0	4.73063	24,740
	2.0	4.97107	26,000
	3.0	5.19612	27,175
	4.0	5.40748	28,280

Figure 10.--*Critical buckling stresses for alternative shear blade configurations and uniform prestressing (Example 2). For the calculation of critical buckling stresses the following assumptions were made: 18-inch by 18-inch shear blade (B/A = 1.0), t = 1/4 inch,* $E = 30 \times 10^6$ *psi,* $\mu = 0.3$*, and* $\sigma_e = 5{,}230$ *psi.*

loadings. However, such a figure is nonexistent to our knowledge. Therefore, design judgment must be used to pick a safety factor that would be considered satisfactory.

Thus, to finalize the example we will assume that a prestress factor of 4.0 has been chosen. The uniform prestress magnitude is then calculated from

$$PPS = PK(\sigma_e)$$

$$= (4.0)(5230)$$

$$PPS = 20{,}920 \text{ psi} .$$

SUMMARY AND CONCLUSIONS

Shear blades have generally not been widely accepted as a tool for felling sawtimber due to excessive splitting damage in the butt log adjacent to the sheared face. Research has shown that splitting damage and force requirements can be reduced by decreasing blade thickness. However, a major problem exists with thin shear blades--they have limited structural stability. Even though the yield point of the blade material has not been reached the plate can buckle laterally and ultimately fail.

Methods to analyze thin rectangular plates for load carrying capacity are highly theoretical and extremely difficult and time consuming to calculate. A versatile computer program has been written[1] to analyze the elastic stability of thin rectangular plates subjected to in-plane compressive loadings with varying boundary conditions. The computer program is also capable of determining the effectiveness of various prestress configurations for increasing plate stability.

Several rectangular plate configurations, prestress conditions, and boundary conditions are discussed in this paper to show that thin plate solutions can be used to approximate thin shear blade configurations. Critical buckling constants have been presented for numerous plate problems as a measure, or indicator, of plate stability. We have shown how the elastic stability of thin rectangular plates can be increased by several prestressing alternatives.

By way of formulas and examples, we have demonstrated how the design engineer can use the results of this analysis to mathematically analyze thin shear blades and to estimate expected critical buckling loads. Further, we have shown how the blade stability can be increased by changing boundary or clamping conditions and by prestressing the blade.

Plate problems of more general applicability, some of which had no previous solutions, are included in Appendix C.

An otherwise very complicated problem has been reduced to a very simple checkout and design procedure that a design engineer can follow to estimate the stability of thin shear blades and methods to increase elastic stability. The foregoing analysis is recommended as a starting point in thin shear blade design.

APPENDIX A

Analysis of the Instability of Thin Rectangular Plates Using the Extended Kantorovich Method[1]

The extended Kantorovich method is used to obtain solutions to a large number of previously unsolved elastic buckling problems of thin rectangular plates. In the present work this method is specially adapted to a numerical method of solution. Earlier workers have applied the Kantorovich method to a small number of plate buckling problems but have not used numerical methods of solution.

The classical Kantorovich method involves reducing the problem of minimization of a double integral, the plate potential, to the problem of minimizing a single integral. This is accomplished by using the Galerkin method and expressing the plate equilibrium equation in terms of its Galerkin equation. The deflection surface of the plate is then assumed to be expressible in terms of two separable deflection functions. One of these functions is then assumed *a priori* such that it satisfies boundary conditions, and the remaining unknown function is sought such that the plate potential is a minimum. This results in a fourth order ordinary differential equation which must be satisfied by the unknown deflection function. Solution of the resulting ordinary differential equation gives an eigenfunction for which the corresponding eigenvalue, the critical or buckling stress, can be found by using the plate boundary conditions.

The extended Kantorovich method used in this work is an iterative version of the classical Kantorovich method. Instead of quitting after finding the first approximation to the critical stress based on an *a priori* assumed deflection function, the extended Kantorovich method uses the newly determined deflection function as a trial function in the same manner that the *a priori* chosen function was used. As a result of this, a new approximate critical stress value can be found. This process can be repeated until the approximate critical stress value converges to some value near the exact solution.

In this work the extended Kantorovich method is used to solve buckling problems of plates having a variety of different varying in-plane stress distributions. To make this possible, numerical methods of solution are employed. A Simpson's rule technique is used to determine the integral constants of the fourth order ordinary differential equation mentioned above. The resulting ordinary differential equation, which in general has nonconstant coefficients, is solved by using a numerical technique for solving boundary value problems. This technique reduces the fourth order ordinary differential equation to a system of first order ordinary differential equations. The equations are then solved using a special version of Hamming's modification of Milne's predictor-corrector method.

The solution method is verified by solving a large number of plate buckling problems with known classical solutions. For problems with known exact solutions the numerical program developed is shown to give the exact solutions. Excellent correlation is also found by comparing solutions with known approximate solutions.

Included among the new problems solved are plates with mixed boundary conditions, plates on elastic foundations, and plates with a variable in-plane compressive load applied to only one edge, together with several different in-plane prestress configurations to increase the magnitude of the critical stress. Information from the results for the prestressed plates is of direct interest to equipment designers for use in the design of thin shear blades for cutting logs. Solutions are also found for plates with beam type stress distributions. Based on these new solutions an evaluation is made of the limitations of previous solutions found using deep beam theory.

APPENDIX B

Legend of Symbols

A = one-half the plate length (in.).

B = one-half the plate height (in.).

B/A = plate aspect ratio (dimensionless).

CKA = buckling constant for A dimension, $CKA=\frac{\sigma_{cr}\ t\ (2A)^2}{\pi^2 D}$ (dimensionless).

CKB = buckling constant for B dimension, $CKB=\frac{\sigma_{cr}\ t\ (2B)^2}{\pi^2 D}$ (dimensionless).

σ_{cr} = critical buckling stress which is the lowest peak applied stress for which the plate has two equilibrium configurations--the initial flat configuration and an infinitesimally deflected configuration--(psi).

t = plate thickness (in.).

D = flexural rigidity of the plate, $D=\frac{Et^3}{12(1-\mu^2)}$ (in.-lbs).

E = modulus of elasticity (psi).

μ = Poisson's ratio (dimensionless).

σ_e = plate stress constant (psi), $\sigma_e=\frac{\pi^2 D}{t(2A)^2}$.

PK = prestress factor, PK=(PPS)/σ_e .

PPS = peak prestress magnitude (psi).

P_c = total (in-plane) force on a plate which is assumed to have a cosine plate stress distribution (lbs), $P_c=\frac{2}{\pi}(2A)t\sigma_c$.

σ_c = peak stress for a cosine distributed load (psi).

P_u = total (in-plane) force on a plate which is assumed to have a uniform plate stress distribution (lbs), $P_u=(2A)t\sigma_u$.

σ_u = uniform stress (psi).

σ_{avg} = estimated average plate stress (psi), $\sigma_{avg}=\frac{\text{total plate force}}{t(2A)}$.

L = smaller value of the two primary plate dimensions (in.).

K = elastic foundation stiffness (psi per inch).

FK = elastic foundation modulus factor.

n = number of half waves in y direction.

APPENDIX C

Buckling Constants for Alternative Rectangular Plate Configurations

The buckling constants in this appendix are included for general reference and to demonstrate the capability of the computer program developed for solving buckling problems of plates having an assortment of boundary conditions and loading distributions. Some of the cases given were previously unsolved.

Figures 11 and 12 show plate configurations which have known exact and approximate classical solutions respectively. These cases were solved as a verification of the solution method used[1] These two figures include drawings of the plate configurations, the Kantorovich solutions found, and the known classical solutions

Case No.	Plate Configuration	B/A	Kantorovich Sol'n CKA	Exact Sol'ns CKA
1	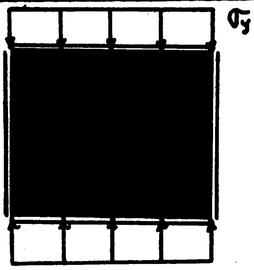	1.0	3.99995	4.0
		1.414	4.49017	4.50
		2.0	3.99999	4.0
2	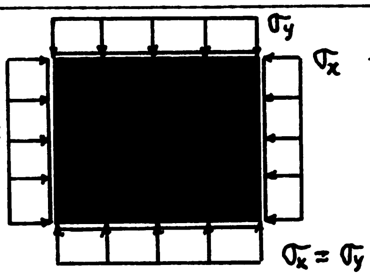	1.0	1.99999	2.0
3	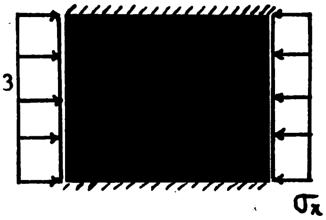	1.0	7.69128	7.692
				7.690
4	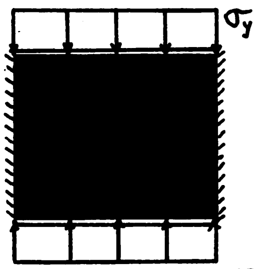	1.0	7.69094	7.692
				7.690
5	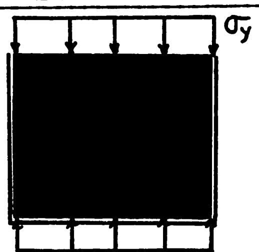 $\mu = 0.3$	0.658	2.31005	2.31

(Figure 11 continued on next page)

Figure 11.--*Verification with known classical exact solutions. Cases 1, 2, 5, and 6 refer to Timoshenko and Gere (1961), cases 3 and 4 to Flugge (1962) and Masao (1969), and cases 7, 8, 9, and 10 to Flugge (1962).*

along with literature citations from which the classical solutions were found. Again a comparison of the Kantorovich results and the classical solutions serves as a verification of the accuracy and dependability of the method used here.

(Figure 11 continued)

Case No.	Plate Configuration	B/A	Kantorovich Sol'n CKA	Exact Sol'n CKA
6	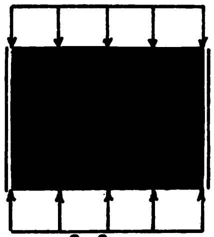 μ = 0.3	0.5	1.58205	1.60
		1.0	2.04294	2.06
		1.316	2.31071	2.31
		2.0	2.26069	2.20
7	 μ = 0.3	0.33	1.29120	1.289
		0.4	1.38522	1.385
		0.67	1.29120	1.289
		1.0	1.65251	1.658
8	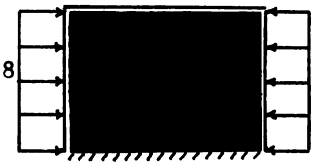	1.0	5.74021	5.74
9	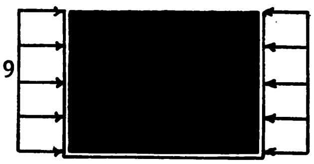 μ = 0.3	1.0	1.4016	1.402
10	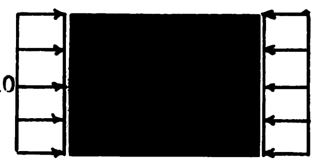 μ = 0.3	1.0	0.95231	0.952

The solutions given in figure 13 are presented to show how the results found in this work compare with "deep beam" solutions for four different plate configurations. All of the cases in figure 13 have beam-like dimensions with respect to length-height ratios, but qualify as thin plates if the thickness is small enough in comparison with

Case No.	Plate Configuration	B/A	Kantoro-vich CKA	Classical Approx. CKA
1	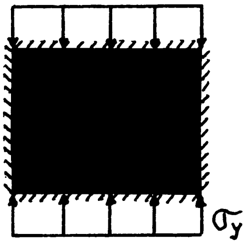	1.0	10.09468	10.07
2	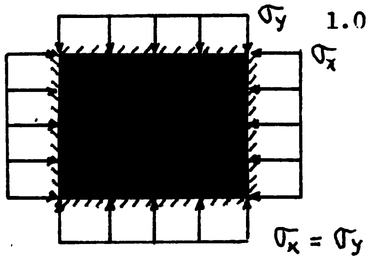	1.0	5.31427	lower boundary 5.30 upper boundary 5.33
3	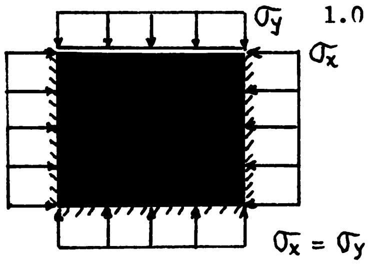	1.0	4.31658	4.3144
4	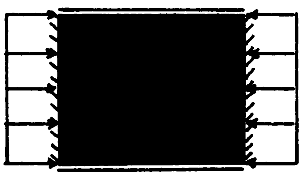	1.0	6.74246	6.74
5	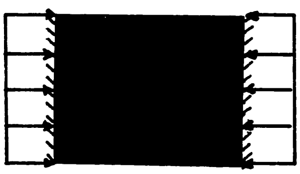	1.0	3.94340	3.928
	$\mu = 0.3$			

Figure 12.--*Verifications with known approximate classical solutions. Cases 1, 4, and 5 refer to Flugge (1962), case 2 refers to Timoshenko and Gere (1961), and case 3 refers to Masao* et al. *(1969). (All results from the Kantorovich CKA are from the fourth iteration).*

Case No.	Plate Configuration	B/A	Kantorovich CKA	Deep Beam Sol'n CKA
1	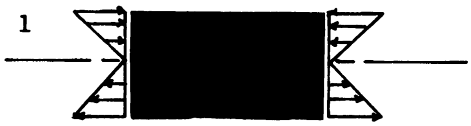 $\mu = 0.3$	0.25	8.75170	8.57953
2	 $\mu = 0.3$	0.25	19.37212	17.15906
3	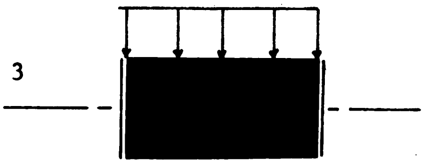 $\mu = 0.3$	0.25	0.65953	0.80506 D.B. Sol'n for load at center line
4	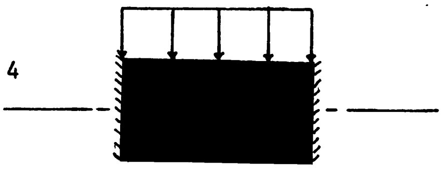 $\mu = 0.3$	0.25	1.24944	1.23177 D.B. Sol'n for load at center line

Figure 13.--*Verification with deep beam solutions. All cases refer to Flugge (1962).*

the other dimensions. The Kantorovich solutions for these cases were higher than the deep beam solutions for all cases except case 3. It is expected, however, that the Kantorovich solutions based on thin plate theory are more accurate than the "deep-beam" solutions based on the more simple beam theory.

Figure 14 shows plate configurations which include three different prestress distributions applied to the vertical edges. These cases with prestressing are all new solutions. A comparison of the results shows the relative effectiveness of the three different prestress distributions for the given plate configurations.

A

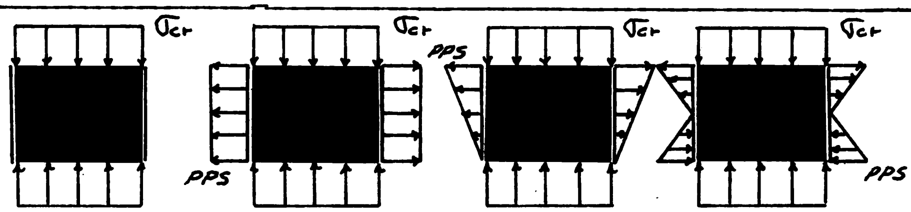

B/A	CKA	CKA	CKA	CKA
0.5	1.60	1.78025	1.60582	1.60510
1.0	2.10	2.66409	2.28612	1.69322
2.0	2.16	2.73375	2.44965	2.67556

PPS = σ_e $\mu = 0.3$

B

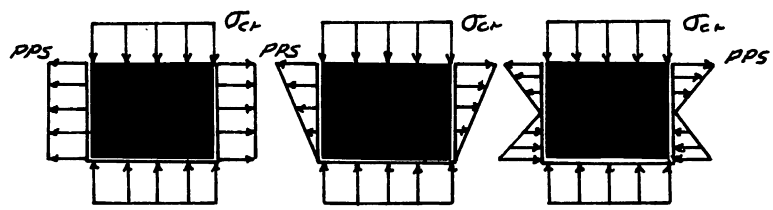

B/A	PK	CKA	CKA	CKA
0.658	0.0	2.31005	2.31005	2.31005
	1.0	2.93043	2.57187	2.76633
	2.0	3.30538	2.79518	3.12952
	3.0	3.56658	2.98371	3.39728

$\mu = 0.3, \ \sigma_e = \dfrac{\pi^2 D}{t\,(2A)^2}$, CKA $= \dfrac{\sigma_{cr}\ t\ (2A)^2}{\pi^2\ D}$, PPS = PK σ_e

Figure 14.—*Prestressed plates with (A) two free edges and (B) one free edge.*

The two plate buckling problems given in figure 15 are for plates resting on linearly elastic foundations, i.e., the deflection of the plate at any point is resisted by a pressure proportional to the deflection. The buckling constant CKA is given for both plates for a range of elastic foundation stiffness values. The first case, with all four edges simply supported, has a known analytical solution. Excellent agreement was obtained between the buckling constants found using the computer program developed in this work and the buckling constants calculated using the known analytical solution. A previously known solution could not be found for the second case in figure 15—a plate with all four edges clamped.

Figure 16 includes four different plate configurations, all of which are loaded by a cosine-shaped in-plane load applied

Plate Configuration	B/A	FK $\left(K=\frac{FK \times \sigma_e}{B}\right)$	n	CKA	Known Analytical Solution
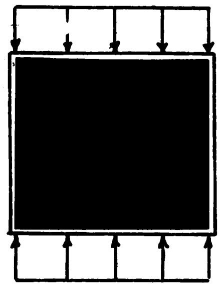	1.0	-0.2	1	-0.03576	-0.03573
		-0.1	1	1.98214	1.98214
		0.0	1	3.99995	4.00000
		0.05	1	5.00876	5.00893
		0.10	1	6.01754	6.01786
A = B = 1.0" , t = 0.02"		0.20	2	7.25855	7.25894
μ = 0.3 , E = 30×10^6psi		0.30	2	7.76330	7.76340
		0.40	2	8.26774	8.26787
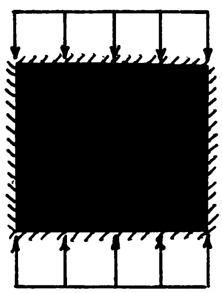	1.0	-0.6	1	0.97994	
		-0.5	1	2.61002	
		-0.4	1	4.20788	
		-0.3	1	5.76603	
		-0.2	1	7.27511	
		-0.1	1	8.72306	
		0.0	1	10.09468	
A = B = 1.0" , t = 0.02"		0.1	1	11.36555	
μ = 0.3 , E = 30×10^6psi		0.2	2	12.52188	
		0.3	2	12.77076	
		0.4	2	13.21331	
		0.5	2	13.62440	

Figure 15.—*Elastic foundation solutions (in equation, K = elastic foundation modulus and FK = elastic foundation modulus factor; n = number of half waves in y direction; known analytical solutions were calculated using equation given in Bulson (1969)).*

to the top plate edge. Cases 1 and 2 are supported at all edges, case 1 with all edges simply supported and case 2 with all edges clamped. Cases 3 and 4, however, are supported at only two edges. These cases both resemble shear blade type configurations; in fact case 4 is the same as case 2 of figure 3. The only difference is that in figure 16 the buckling constant CKB is given along with the buckling constant CKA.

Case No.	Plate Configuration	B/A	$CKA = \frac{\sigma_{cr}\ t\ (2A)^2}{\pi^2\ D}$	$CKB = \frac{\sigma_{cr}\ t\ (2B)^2}{\pi^2\ D}$
1	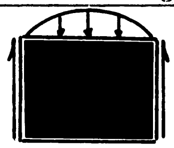	0.5	12.20898	3.05224
		1.0	7.38091	7.38091
		2.0	7.20327	28.81308
2	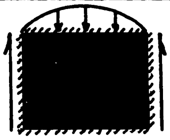	0.5	36.10814	9.02703
		1.0	19.09650	19.09650
		2.0	17.76844	71.07375
3	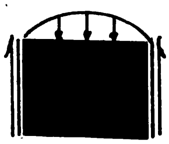	0.25	0.87438	0.05465
		0.33	1.09146	0.11886
		0.50	1.50201	0.37550
		0.67	1.78303	0.80040
		0.75	2.00720	1.12905
		1.0	2.10034	2.10034
		1.5	2.20323	4.95726
		2.0	2.21380	8.85519
	$\mu = 0.3$	3.0	2.21470	19.93233
4	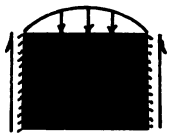	0.25	1.57461	0.09841
		0.33	2.00768	0.21864
		0.50	2.81051	0.70263
		0.67	3.33195	1.49571
		0.75	3.50014	1.96882
		1.0	3.82011	3.82011
		1.5	3.92528	8.83188
		2.0	3.94223	15.76893
	$\mu = 0.3$	3.0	3.94124	35.47114

Figure 16.--*Plates loaded on one edge.*

LITERATURE CITED

Arola, R. A. 1971. Crosscut shearing of roundwood bolts. USDA For. Serv. Res. Pap. NC-68, 21 p., illus. North Cent. For. Exp. Stn., St. Paul, Minn.

Arola, R. A. 1972. Estimating force and power requirements for crosscut shearing of roundwood. USDA For. Serv. Res. Pap. NC-73, 8 p., illus. North Cent. For. Exp. Stn., St. Paul, Minn.

Bulson, P. S. 1969. The stability of flat plates. 470 p. New York: American Elsevier Publishing Co.

Flugge, W., ed. 1962. Handbook of engineering mechanics. New York: McGraw-Hill Book Co.

Masao, Y., K. Masatsuga, N. Takao, H. Shigeru, S. Makota, and H. Atsushi. 1969. Handbook of elastic stability. Revised and supplemented, NASA TT F-12, 172, Washington, D.C. 686 p.

McIntosh, J. A., and E. L. Kerbes. 1968. Tree shears reduce felling costs, offer other savings. Can. For. Ind. 88(3): 42-47, illus.

Schmidt, O. A., and R. E. Melton. 1968. Felling white pine saw timber trees with a hydraulic shear causes loss of lumber in butt logs. The Northern Logger and Timber Processor. 16(11): 22, 23, 40, illus.

Timoshenko, S. P., and J. M. Gere. 1961. Theory of elastic stability. Ed. 2, 541 p. New York: McGraw-Hill Book Co.

Wiklund, Martin. 1967. Forces and damage in felling and buckling with knife and shear type tools. Report 9, Forskningsstiftelsen Skogsarbeten, Stockholm, Sweden. p. 39.

☆U.S. Government Printing Office: 1974 — 762-867